Solid-State ^{2}H NMR Shows Equivalence of Dehydration and Osmotic Pressures in Lipid Membrane Deformation

K. J. Mallikarjunaiah,[†] Avigdor Leftin,[†] Jacob J. Kinnun,[‡] Matthew J. Justice,[§] Adriana L. Rogozea,[§] Horia I. Petrache,[§] and Michael F. Brown[†‡*]

[†]Department of Chemistry and [‡]Department of Physics, University of Arizona, Tucson, Arizona; and [§]Department of Physics, Indiana University-Purdue University Indianapolis, Indianapolis, Indiana

ABSTRACT Lipid bilayers represent a fascinating class of biomaterials whose properties are altered by changes in pressure or temperature. Functions of cellular membranes can be affected by nonspecific lipid-protein interactions that depend on bilayer material properties. Here we address the changes in lipid bilayer structure induced by external pressure. Solid-state ^{2}H NMR spectroscopy of phospholipid bilayers under osmotic stress allows structural fluctuations and deformation of membranes to be investigated. We highlight the results from NMR experiments utilizing pressure-based force techniques that control membrane structure and tension. Our ^{2}H NMR results using both dehydration pressure (low water activity) and osmotic pressure (poly(ethylene glycol) as osmolyte) show that the segmental order parameters (S_{CD}) of DMPC approach very large values of $\approx$0.35 in the liquid-crystalline state. The two stresses are thermodynamically equivalent, because the change in chemical potential when transferring water from the interlamellar space to the bulk water phase corresponds to the induced pressure. This theoretical equivalence is experimentally revealed by considering the solid-state ^{2}H NMR spectrometer as a virtual osmometer. Moreover, we extend this approach to include the correspondence between osmotic pressure and hydrostatic pressure. Our results establish the magnitude of the pressures that lead to significant bilayer deformation including changes in area per lipid and volumetric bilayer thickness. We find that appreciable bilayer structural changes occur with osmotic pressures in the range of 10−100 atm or lower. This research demonstrates the applicability of solid-state ^{2}H NMR spectroscopy together with bilayer stress techniques for investigating the mechanism of pressure sensitivity of membrane proteins.

INTRODUCTION

Water is the essence of life on Earth and the hydrophobic effect (1) provides an important driving force for the self-assembly of biomolecules, including both proteins and lipids in biomembranes (2–6). Altering the activity of aqua vitae has profound effects on drought-tolerant plants (7) and animals (8), as well as biomembrane constituents including aquaporins (9), mechanosensitive channels (10,11), and G protein-coupled receptors (12,13). Lipid bilayers are elastic materials (14,15) and can undergo significant deformation in response to stress, whereby nonspecific material properties govern protein-mediated functions of cellular membranes (16). The interactions of lipids include a balance of attractive long-range van der Waals forces with shorter-range repulsive forces that together govern their micro- or nanostructures. Water and osmotic stress may indirectly affect function due to structural changes of the biomembrane (16), and there may also be direct effects on membrane proteins (17). A chemically nonspecific stress field within the membrane (16) may underlie bilayer strain-induced changes in protein activity in terms of elastic constants (moduli) described by a flexible surface model (16,18,19).

Membrane structural changes due to bilayer stress can be explored in three different ways: application of dehydration pressure by gravimetrically adding a controlled amount of water (20,21) (Fig. 1 *a*); osmotic pressure involving the addition of osmolyte (22) (Fig. 1 *b*); or by directly applying hydrostatic pressure (23–25) (Fig. 1 *c*). Each method is thermodynamically related, because the molar work of transfer of water from the interlamellar space corresponds to a reduction in chemical potential (μ_W) that is balanced by the external pressure (Π or P). As discussed by Israelachvili and Wennerström (26), the repulsive interbilayer pressure (27) is attributed to undulations that provide an entropic force over large length scales, and at shorter distances either to an exponentially decaying hydration force (28,29), or to entropic protrusion forces between fluctuating lipids. (The dehydration pressure should not be confused with the so-called hydration force (29), because it also includes a steric component (26,27)). Although the theoretical equivalence of osmotic pressure and gravimetric dehydration is well understood (29,30), the extent of membrane deformation is less clear (28,31), because different experimental approaches lead to varying conclusions (29,31–34). According to Koenig et al. (22), the discrepancy may entail applying the so-called Luzzati method—which combines gravimetric, volume, and small-angle x-ray scattering measurements to obtain the unit cell dimensions—versus use of electron density profiles to determine the structure within the unit cell (28,31,35). Because hydration variation is typically used to solve the phase problem in x-ray studies

Submitted July 4, 2010, and accepted for publication November 8, 2010.

*Correspondence: mfbrown@u.arizona.edu

Editor: Klaus Gawrisch.

0006-3495/11/01/0098/10 $2.00

doi: 10.1016/j.bpj.2010.11.010

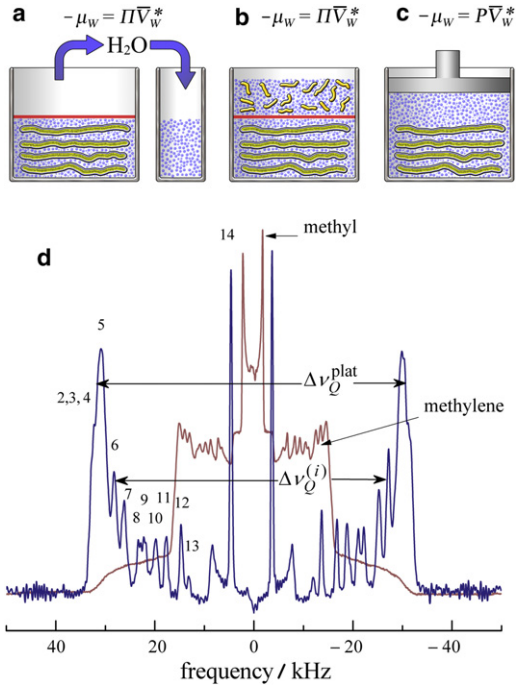

FIGURE 1 Investigation of lipid bilayer interactions by solid-state ^{2}H NMR spectroscopy. A schematic representation of three different ways of applying pressure is shown. (*a*) Dehydration pressure (Π) is created by gravimetrically removing water from lipids at full hydration and is equivalent to transfer across a virtual membrane. (*b*) Osmotic pressure (Π) is due to addition of osmolyte and involves removal of water across a semipermeable membrane (solid horizontal line) shown at the center. (*c*) Hydrostatic pressure (P) applied directly leads to displacement of interlamellar water due to the anisotropic bilayer compressibility. In each case, the contribution to the free energy of water due to changing the pressure is indicated by the corresponding chemical potential μ_W where $\overline{V}_W \approx \overline{V}_W^*$ is the partial molar volume of water and $\overline{V}_W^*$ is the molar volume. (*d*) Representative solid-state ^{2}H NMR powder-type spectrum (*thin line*) and de-Paked spectrum (*thick line*) for multilamellar dispersion of DMPC-d_{54} with perdeuterated acyl groups. The sharp peaks of the powder-type ^{2}H NMR spectrum of randomly oriented bilayers originate from the $\theta = 90°$ orientation. The de-Paked spectrum corresponds to the $\theta = 0°$ orientation and gives a twofold increase and sign reversal of the splittings. The residual quadrupolar couplings are designated by $\Delta\nu_Q^{(i)}$ and yield the order parameters $|S_{CD}^{(i)}|$ of the C−^{2}H bonds directly, where $i = 2\ldots14$ is the acyl chain segment index.

(35), the influences of membrane deformation could also potentially affect the form factors and derived structures.

Here we apply solid-state ^{2}H NMR spectroscopy (36) as an experimental counterpart to x-ray studies (22,29,30,32,37–39) that have led to seminal insights into the role of water in membrane organization. Compared to x-ray diffraction (35,40) or micropipette deformation (41), ^{2}H NMR has the considerable advantage of being able to probe bilayer properties at a site-specific level in terms of individual lipid segments (42,43). Fig. 1 *d* shows how the residual quadrupolar couplings in ^{2}H NMR spectroscopy are connected with the average bilayer structure using phospholipids uniformly deuterated along the acyl chains. Mobility of the lipids as well as collective lipid motions due to steric forces are detected over a broad range of time and distance scales (14,44). Any change in thermodynamic state variables is manifested by the quadrupolar splittings $\Delta\nu_Q^{(i)}$ via the segmental order parameters, which are crucial for testing the validity of force fields in molecular dynamics studies (15,45,46). Equivalence of dehydration and osmotic pressure (29) is shown by treating the NMR machine as a virtual osmometer, which enables comparison of the results with reported hydrostatic data (23,47). Most strikingly, we find evidence of significant bilayer structural changes from the ^{2}H NMR order parameters over the entire range of osmotic pressures investigated (0–230 atm). The correspondence of interbilayer repulsive pressure induced osmotically (22) to structural changes by direct application of hydrostatic pressure (47) is then examined. We explain how the comparatively small changes induced by hydrostatic pressures ($\approx$1000 atm) are mainly due to squeezing water from the interlamellar space. This process is far less efficient than direct removal of water by dehydration or osmotic stress. Last, we point out the implications for conformational changes of pressure-sensitive membrane proteins, including G protein-coupled receptors like rhodopsin as well as mechanosensitive ion channels.

EXPERIMENTAL METHODS

1,2-diperdeuteriomyristoyl-*sn*-glycero-3-phosphocholine (DMPC-d_{54}) was obtained from Avanti Polar Lipids (Alabaster, AL) and lyophilized from hexanes to constant weight. The number of waters per lipid was calculated using their gravimetric proportion of weights. For the osmolyte method, an appropriate quantity of poly(ethylene glycol) (M_r 1500) (PEG 1500) (Sigma-Aldrich, St. Louis, MO) was added to the lipids after the lyophilization step. Osmotic pressure measurements were carried out as described in the Supporting Material. Solid-state ^{2}H NMR measurements were conducted using an AMX-300 spectrometer (Bruker, Billerica, MA) operating at 7.05 T (^{2}H frequency of 46.07 MHz). Spectral assignments for DMPC-d_{54} were made by integration of de-Paked resonances (48) (see Fig. 1 *d*). The order parameters, S_{CD}, were evaluated using the relation (42)

$$\left|\Delta\nu_Q^{(i)}\right| = \frac{3}{2}\chi_Q \left|S_{CD}^{(i)}\right|\left|P_2(\cos\theta)\right|. \quad (1)$$

Here, $\Delta\nu_Q^{(i)}$ is the experimental ith quadrupolar splitting, where $\chi_Q \equiv e^2qQ/h = 167$ kHz is the static quadrupolar coupling constant, and $P_2(\cos\theta) = (1/2)(3\cos^2\theta - 1)$, where θ is the angle between the membrane director and the static magnetic field. For random multilamellar lipids, $\theta = 90°$, leading to $P_2(\cos\theta) = -1/2$; and for the de-Paked ^{2}H NMR spectra, $\theta = 0°$, yielding $P_2(\cos\theta) = 1$ (42). The segmental order parameters are given by

$$S_{CD}^{(i)} = \frac{1}{2}\left\langle 3\cos^2\beta_i - 1\right\rangle, \quad (2)$$

where β_i is the instantaneous angle between the C−^{2}H bond and the membrane normal, and the angular brackets indicate a time-ensemble average. They are related to the bilayer mean area per lipid $\langle A\rangle$ and to the volumetric thickness per monolayer D_C in terms of a mean-torque model (49). Full experimental details are included in the Supporting Material.

RESULTS

Deuterium NMR spectroscopy shows pressure-induced changes of DMPC membranes

Representative de-Paked ^{2}H NMR spectra at $T = 35°C$ corresponding to gravimetrically prepared DMPC-d_{54} samples with different water/lipid ratios (50, 40, 30, 20, 10, 6.8, and 3.1 wt % H_2O) are presented in Fig. 2 *a*. Inspection of the peak positions demonstrates that the maximum quadrupolar splitting does not change appreciably from 50 wt % H_2O (52.34 kHz, $n_{W/L} = 41$) to 30 wt % H_2O (53.80 kHz, $n_{W/L} = 18$). However, further decreasing the water content begins to stress the membrane noticeably, as evinced by an increase in the quadrupolar splittings. From 30 wt % H_2O (53.80 kHz, $n_{W/L} = 18$) to 20 wt % H_2O (60.25 kHz, $n_{W/L} = 10$), there is a loss of eight waters per lipid, with an increase of the maximum quadrupolar splitting of 6.45 kHz.

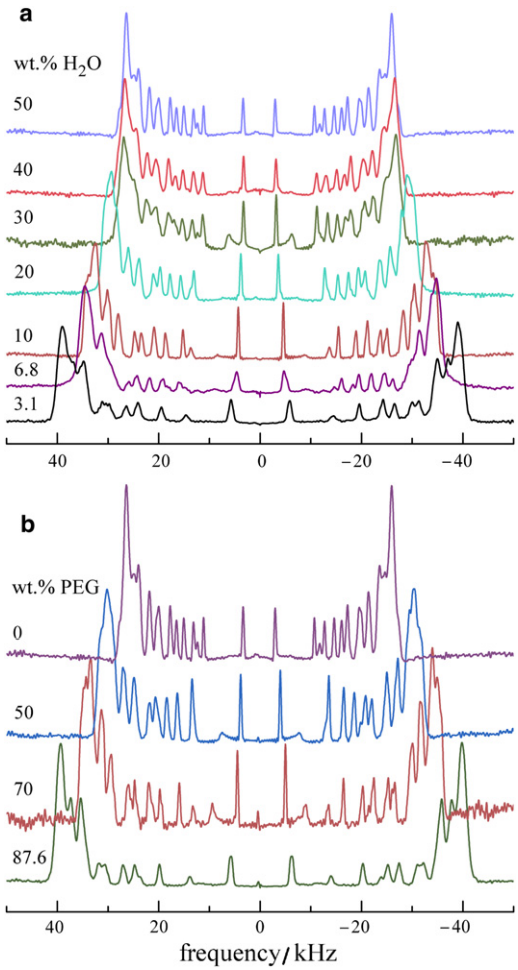

FIGURE 2 Solid-state ^{2}H NMR de-Paked spectra in the liquid-crystalline (liquid-disordered or L_α) state at $T = 35°C$ for DMPC-d_{54} bilayers showing the effect of (*a*) different amounts of hydration water and (*b*) various concentrations of osmolyte poly(ethylene glycol) M_r 1500 (PEG 1500). In both cases, the quadrupolar splittings (peak-to-peak splitting) $\Delta\nu_Q^{(i)}$ change due to removal of water from the interlamellar space.

The trend of an increase of quadrupolar splittings with a decrease in $n_{W/L}$ continues significantly, with the highest value for 3.1 wt % H_2O (77.99 kHz, $n_{W/L} = 1.34$). In Fig. 2 *b*, de-Paked ^{2}H NMR spectra at $T = 35°C$ corresponding to samples of DMPC-d_{54} with different concentrations of osmolyte (0, 50, 70, and 87.6 wt % PEG 1500) are shown. Focusing on the maximum (plateau) quadrupolar splitting of the lipid acyl chains, a striking increase is seen as the concentration of osmolyte (osmotic pressure) increases. In the absence of PEG 1500 ($n_{W/L} \approx 41$), the quadrupolar splitting of the plateau peak position is 52.34 kHz, which increases to 79.07 kHz at 87.6 wt % PEG. Osmotic pressure values corresponding to osmolytes with different relative molar masses (M_r) have been tabulated (50), and additional measurements are given in the Supporting Material.

Phospholipid membrane structure is altered by dehydration or osmotic stress

Next, Fig. 3, *a* and *b*, presents a comparison of the segmental order parameter profiles at $T = 30°C$ for the gravimetric and osmolyte samples, respectively. Striking increases in the order profiles are seen due to lipid membrane dehydration or osmotic stress, whereas the segmental order parameters increase $\approx$ uniformly at each position. The largest values are observed for the PEG 1500 and gravimetric samples at an equivalent $n_{W/L} = 1.34$ (see below). Maximum order parameters for plateau acyl chain segments of 0.337 are observed, which approach those seen with addition of cholesterol (51,52). The lowest values correspond to excess interlamellar water and are found to be 0.211 (at $n_{W/L} = 41$) for the plateau peak position. The excellent correspondence of the segmental order profiles of DMPC-d_{54} due to decreasing H_2O or addition of PEG 1500 demonstrates that the two approaches are fundamentally equivalent. In both cases, the removal of H_2O yields a similar variation for the various segmental positions along the acyl chains.

Membrane stress is affected by changing temperature

For all the samples, de-Paked ^{2}H NMR spectra and corresponding segmental order parameter profiles were measured as a function of temperature (30, 35, 45, 50, and 65°C; results not shown). A reduction in the order parameter profiles is seen with increasing temperature, as discussed by Petrache et al. (49) in terms of the isobaric thermal expansivity due to increased bilayer area and diminished volumetric thickness. Representative data for DMPC-d_{54} containing 20 wt % H_2O at all temperatures are presented in the Supporting Material. The DMPC membrane system has a gel-to-liquid-crystalline phase transition temperature (T_M) of 23°C (53), which for DMPC-d_{54} is reduced to 19.5°C by deuteration.

To establish that the effects of dehydration or osmotic stress are not due to changes in T_M values, we acquired

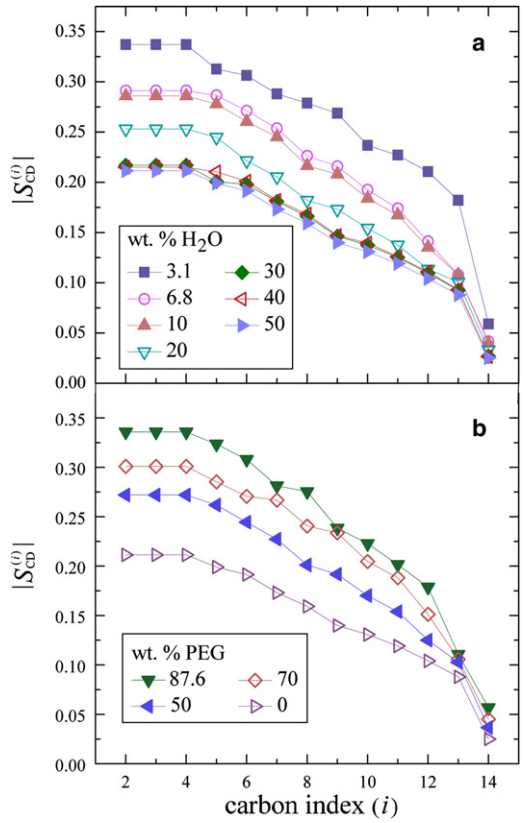

FIGURE 3 Segmental order parameters $|S_{CD}^{(i)}|$ as a function of acyl chain segment index (i) for DMPC-d_{54} bilayers in the liquid-crystalline (L_α) state at $T = 30°C$. (*a*) Order profiles with different wt % H_2O as determined gravimetrically represent dissimilar dehydration pressures (symbols defined in figure). (*b*) Order parameter profiles as a function of wt % PEG 1500 corresponding to various osmotic pressures (see figure for symbol definitions). Removal of water yields a large increase in $|S_{CD}^{(i)}|$ values due to interbilayer steric interactions and/or membrane deformation, involving an increase in volumetric thickness D_C together with a reduction in lipid cross-sectional area $\langle A \rangle$.

^{2}H NMR spectra of the samples in the vicinity of the phase transition temperature (results not shown). The data indicate a maximum increase in T_M to $\approx 30°C$ for 3.1 wt % H_2O (as well as for the 87.6 wt % PEG 1500) sample. Similar small shifts in DMPC phase transition temperatures have been observed under hydrostatic pressure (24). We conclude that the dramatic changes in ^{2}H NMR splittings and order profiles are a direct consequence of dehydration or osmotic pressure, and not due to differences in the phase transition temperature (54). Influences of temperature on bilayer structural parameters have also been investigated using x-ray diffraction, and interpreted in terms of a temperature-dependent decrease in the bilayer bending modulus (37).

Membranes can be deformed by applying external pressure in three different ways

The ^{2}H NMR spectra and order parameter profiles corresponding to the three different pressure techniques, namely dehydration (gravimetric), osmotic (PEG 1500 osmolyte), and hydrostatic pressures, at 45°C are shown in Fig. 4. For comparison, we include de-Paked spectra and order parameter measurements as a function of hydrostatic pressure conducted by Brown et al. (47). Notably, for either gravimetrically or osmotically dehydrated samples, there is a striking increase in the segmental order parameters as stress on the membrane is increased. At this temperature, the quadrupolar splittings (order parameter) of the plateau region change from 45.94 (0.183) to 69.41 (0.277) kHz in dehydration and 45.94 (0.183) to 70.19 (0.280) kHz in osmotic pressure studies.

The larger order parameters are indicative of bilayer deformation (strain) involving a reduction in $\langle A \rangle$ and an increase in D_C as water is expelled from the membrane (not shown). Changes in the segmental order parameters are evident for osmolyte concentrations from 0 to 87.6 wt % PEG 1500 and span a pressure range of 22 MPa ($\approx$200 atm). The gravimetric method shows that above 30 wt % H_2O, there is hardly any significant change in order parameters, because the water is distributed between both the membrane partition and bulk water partition. However, removal of water below the full hydration limit of $n_{W/L} \approx 20$ stresses the membrane, causing the lyotropic system to alter its shape at the microscopic level (strain) to maintain the fluidity and integrity of the membrane.

By contrast, in the hydrostatic pressure technique (47), the order parameter $|S_{CD}^{plat}|$ changes only from 47.22 (0.188) to 56.86 (0.227) kHz. This comparison substantiates that even for a hydrostatic pressure of 138.6 MPa, the increase in the order parameters for all segments in the acyl chains is comparatively less than for the dehydration and osmotic pressure methods. In the latter cases, an increase in external pressure yields a striking increase in the order parameters $S_{CD}^{(i)}$, e.g., due to a greater volumetric thickness D_C and a corresponding diminution in lipid cross-sectional area $\langle A \rangle$. Whether similar influences on bilayer properties can be measured with x-ray diffraction experiments remains to be established.

DISCUSSION

Phospholipids dispersed in water form bilayers that are important models for biological membranes. Lipid membranes are not only solvents for proteins, but their composition, structure, and dynamical properties have implications for cellular functions (55). The phospholipid membrane is a lyotropic liquid-crystalline system, and the structural and dynamic properties (22,56–59) are inseparable from the concentration of bulk and hydration water of the membranes (60,61). Notably, lipid bilayer interactions have been studied extensively using osmotic pressure (29,62,63), vesicle adhesion techniques, and other biophysical methods. Studies of membrane-bending deformations reveal that additives such as detergents and cholesterol

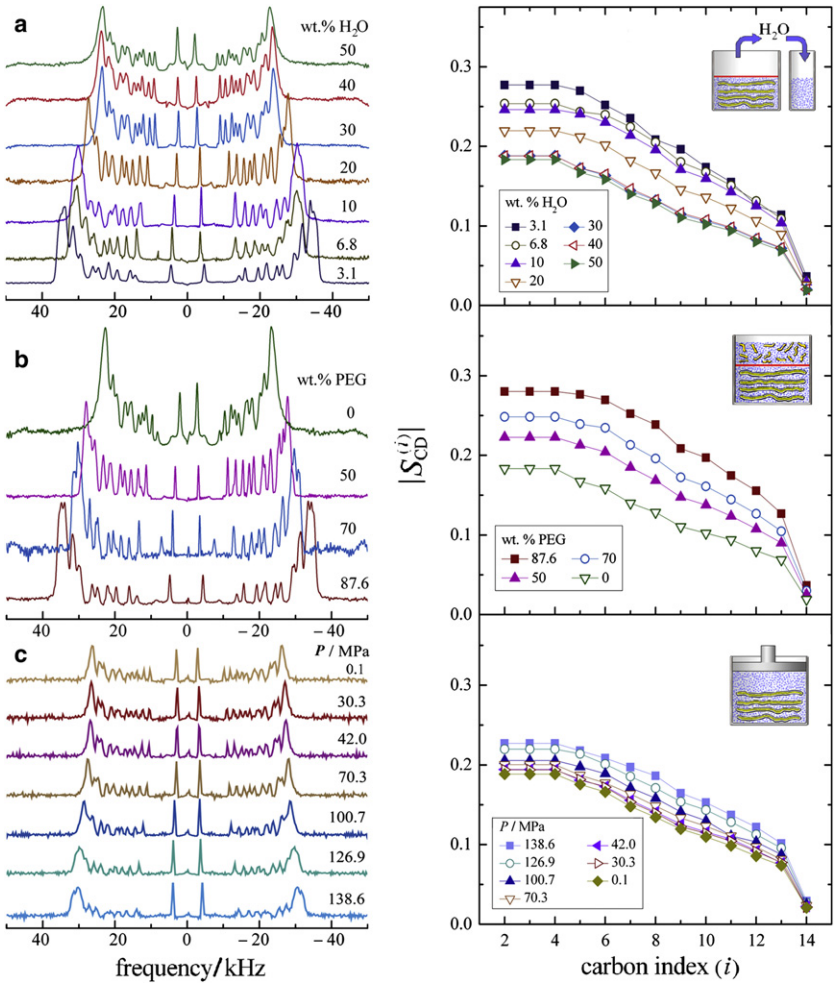

FIGURE 4 Comparison of bilayer structural changes as revealed by solid-state ^{2}H NMR for three different methods of applying external pressure (see Fig. 1, *a*–*c*). Solid-state ^{2}H NMR spectra (*left*) and corresponding C–^{2}H bond segmental order profiles (*right*) are shown as a function of segment index (*i*) for DMPC-d_{54} bilayers in the liquid-crystalline (L_α) state at $T = 45°C$. (*a*) ^{2}H NMR spectra and $|S_{CD}^{(i)}|$ order profiles showing bilayer deformation induced by increased dehydration pressure (gravimetric dehydration). (*b*) ^{2}H NMR spectra and $|S_{CD}^{(i)}|$ order profiles as a function of osmotic pressure due to the presence of PEG 1500. (*c*) ^{2}H NMR spectra and $|S_{CD}^{(i)}|$ order profiles obtained at different bulk hydrostatic pressures (data from Brown et al. (47) with permission of the American Physical Society). Note that a larger change in segmental order profiles is seen with application of dehydration or osmotic pressure than for hydrostatic pressure.

can have a significant influence on the membrane elastic properties (44,64).

As first shown for rhodopsin (65) and reviewed in Brown (16), the bilayer lipid composition (flexible surface model) can affect both the structure and function of membrane proteins (16,18,65). Effects of osmotic stress (activity of water) on the activating conformational change of rhodopsin have also been reported (12,13). Pressure-sensitive proteins, like the mechanosensitive channel of large conductance (66,67), respond to osmotic downshock by undergoing rearrangements of the tertiary fold of the protein to recover cell turgor or relieve excessive internal pressure that may rupture or lyse the cell (11). The importance of lipid interactions in the mechanism of mechanosensitive channel of large conductance has been shown in subsequent work (68,69). Osmotic stress of the membrane bilayer may correspond to the membrane-dependent structural rearrangement of mechanosensitive proteins and changes in conformational equilibrium of membrane proteins due to hydrophobic mismatch (16). In this light, we may consider the membrane lipid bilayer itself as an osmosensor.

Water plays a key role in membrane deformation

How are membrane steric interactions and bilayer structural deformation manifested in experimental biophysical measurements? To expel water from the bilayer, there are mainly two possibilities—either by using direct dehydration, or by removal of water through applying an osmotic or hydrostatic pressure. The effects of pressure and temperature are described by the compressibility and thermal expansivity coefficients (moduli), respectively (49). Hydration of lipids has been investigated extensively (29,70,71), whereby the number of waters per lipid can be controlled by gravimetrically varying the amount of water or addition of osmolyte, which removes water from the interbilayer region. When lipid bilayers are forced into close proximity, short-range repulsion is generated (30,72), including both hydration and steric components (27,31) due to bilayer undulations and/or protrusion forces (26). Addition of osmolyte to the bilayer yields a reduction of interbilayer distance that has been extensively investigated with x-ray diffraction involving Fourier synthesis and small-angle

x-ray scattering experiments (39,73). Parsegian et al. (29) have considered the work of deformation and repulsion of phosphatidylcholine bilayers, and concluded that significant increases in thickness and corresponding decreases in area occur in the range of 50 atm, in agreement with x-ray studies of the Nagle laboratory (74,75). However, these conclusions differ from the work of McIntosh and Simon (28) and McIntosh et al. (31), who find smaller changes in bilayer thickness and area per lipid from electron density profiles. The controlled addition of water has also been studied for different lipids using infrared spectroscopy, calorimetry, NMR (76–78), and molecular dynamics simulations (79).

Now, in previous NMR measurements the quadrupolar splitting of the deuterium nucleus of ^2H_2O has been investigated, providing evidence for different shells of waters between the membrane bilayers (60,78,80). Because the thickness of the lipid headgroup hydration layer is roughly constant (35), the removal of water leads to a reduction of the bilayer aqueous interfacial area $\langle A \rangle$ plus suppression of collective membrane fluctuations (14,44). There is an elastic deformation that involves a corresponding increase of the volumetric thickness per monolayer D_C (49). The area contraction and longitudinal (axial) stretch are inversely related and opposite in direction, and together with Young's modulus are described by the Poisson ratio ($0 < \sigma < 1/2$). Assuming the transverse contraction exceeds the longitudinal stretch, an increase in hydrostatic pressure also leads to expulsion or removal of water from the membrane. Comparison of gravimetrically induced membrane deformations with structural changes caused by osmotic pressure is based on the thermodynamic principle of balancing the chemical potential (73).

Changes in the equilibrium chemical potential of the water or lipids are simply related to the free energy of the chemical species for a thermodynamic system composed of the membrane (lipids and interlamellar water) and bulk water partitions. Equilibration of the membrane against an osmolyte solution involves a difference of pressures between these two partitions. This osmotic pressure acts to remove water from the membrane phase, and stresses the membrane, causing it to deform. In the gravimetric method, the experimentalist physically removes the water from the membrane partition. In essence, the removal of water by the osmolyte solution is the same as the removal of water by the person. Here our fingers—or rather the pipette—take the place of the polymer in solution. In both cases, the chemical potential of the water in the membrane partition increases as water is taken up by the bulk partition. Under increasing membrane stress, work is extracted from the membrane partition, and the free energy of the membrane is minimized.

Dehydration pressure is equivalent to osmotic pressure for lipid membranes

Utilizing solid-state ^2H NMR spectroscopy, an empirical relation between order parameters and the osmotic pressure

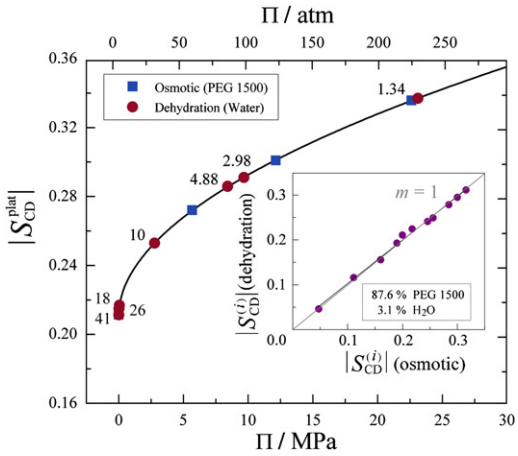

FIGURE 5 Experimental correspondence of dehydration pressure and osmotic pressure for lipid membranes established by solid-state ^2H NMR spectroscopy. Plot of $|S_{CD}^{(i)}|$ values for plateau region of order parameter profile of DMPC-d_{54} at $T = 30°C$ with different concentrations of PEG 1500 osmolyte (■) versus osmotic pressure measured with vapor pressure osmometry. Order parameters $|S_{CD}^{plat}|$ of DMPC-d_{54} at $T = 30°C$ with different hydration levels (●) are equivalent to osmotic pressure in terms of number of waters per lipid $n_{W/L}$ (given next to data points). (*Solid curve*) Fit to the polynomial $|S_{CD}^{plat}| = a + b\,\Pi^c$, where a, b, and c are adjustable parameters. (*Inset*) $|S_{CD}^{(i)}|$ order parameters for the entire acyl chain of DMPC-d_{54} containing 3.1 wt % H_2O (dehydration pressure) plotted versus the corresponding $|S_{CD}^{(i)}|$ values for DMPC-d_{54} with 87.6 wt % PEG 1500 osmolyte (osmotic pressure) at $T = 35°C$. The equivalence of dehydration and osmotic pressure is demonstrated by the slope of $m = 1$.

can be established as shown in Fig. 5. The values of Π for each of the PEG solutions containing DMPC-d_{54} were interpolated from tabulated data obtained by vapor pressure osmometry (see the Supporting Material). The corresponding C−^2H bond order parameters for the gravimetrically dehydrated samples were then matched to the corresponding dehydration (osmotic) pressures (Fig. 5). For example, the inset shows the order parameters for each carbon segment for DMPC-d_{54} containing 3.1 wt % H_2O plotted versus those for DMPC-d_{54} with 87.6 wt % PEG 1500. A straight line with a slope $\approx$ 1 is obtained, thereby substantiating the equivalence between osmotic pressure and dehydration pressure. Similar linear plots were obtained for all the samples investigated in this work, allowing us to match osmotically stressed samples with their dehydrated counterparts (results not shown).

Next, referring back to Fig. 1, *a* and *b*, we see that the gravimetric removal of water or the addition of osmolyte are thermodynamically equivalent in terms of the number of waters per lipid ($n_{W/L}$). Moreover, there is a correspondence to the bulk hydrostatic pressure (P) as described below. We can understand the response of the water and lipid system through consideration of the chemical potential of water μ_W together with the thermodynamic relation $(\partial\mu_W/\partial P)_T = \overline{V}_W$. The osmotic pressure Π is related to the molar ratio of water/lipid $n_{W/L}$ (for constant hydrostatic pressure) by

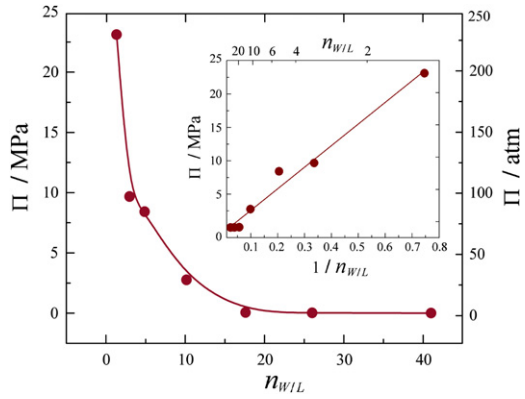

FIGURE 6 Plot of theoretical dehydration pressure (Π) determined from solid-state ^{2}H NMR spectroscopy for DMPC-d_{54} bilayer at $T = 45°C$ as a function of measured number of waters per lipid $n_{W/L}$. (*Inset*) Plot of Π versus the inverse of $n_{W/L}$ showing the predicted linear dependence. The value of the osmotic coefficient φ is calculated from the slope (see Eq. 3).

$$\Pi = \varphi RT/\overline{V}_W n_{W/L}, \tag{3}$$

in which φ is the osmotic coefficient (81). The partial molar volume of water $\overline{V}_W$ is approximated by the molar volume $\overline{V}_W^* = 1/\rho$, where ρ is the density. In Eq. 3, the osmotic coefficient describes the competition of lipid and osmolyte for the solvent, where $\varphi < 1$ is due to lipid interactions with water. For the gravimetric samples, we can directly calculate the number of waters per lipid ($n_{W/L}$), and thereby test the equivalence of dehydration and osmotic pressure for lipid bilayers in Eq. 3.

Fig. 6 shows such a plot of the equivalent dehydration (osmotic) pressure Π as a function of the measured values of $n_{W/L}$, which is a rectangular hyperbola at constant hydrostatic pressure P in accord with Eq. 3. Moreover, the data can be plotted as a function of $1/n_{W/L}$ as shown in the inset, yielding a straight line whose slope gives the osmotic coefficient directly ($\varphi = 0.23 \pm 0.01$). As discussed elsewhere (22,35), the correspondence of gravimetric and osmotic pressure methods may be affected by the extra aqueous volume due to defect regions of the multilamellar lipid dispersion that are equivalent to exerting osmotic pressure. The additional aqueous volume due to defects in multilamellar lipid samples may lead to exaggerated area changes for the unit cell near full hydration. However, the results of Fig. 6 lead us to conclude that solid-state ^{2}H NMR substantiates the theoretical equivalence of dehydration and osmotic pressures (29) for lipid membranes.

Osmotic pressure corresponds to hydrostatic pressure for lipid bilayers

We can also ask the question: what is the connection between osmotic pressure and hydrostatic pressure in lipid membrane deformation? The influence of directly applying hydrostatic pressure to multilamellar lipid dispersions in excess water has been investigated by Brown et al. (47) and Bonev and Morrow (82) using solid-state ^{2}H NMR spectroscopy. In contrast to earlier hydrostatic pressure experiments of Parsegian et al. (29,73), water is not allowed to escape across a dialysis membrane—hence, there is not a direct equivalence to osmotic pressure, as in our measurements and in the work of Koenig et al. (22). Compared to our results for osmotic pressure in Fig. 4, *a* and *b*, the effects of hydrostatic pressure are much smaller in Fig. 4 *c*—why is this? Referring to Fig. 1 *a*, we see there is a correspondence between the hydrostatic pressure (P) acting directly upon lipid membranes and equivalent osmotic pressure (Π) through the molar ratio of water/lipid ($n_{W/L}$). The origin can be traced back to the fact that for a lipid bilayer the transverse (area or lateral) compressibility is greater than the longitudinal (length or axial) compressibility when the Poisson ratio σ is between 0 and 1/2. Due to the anisotropic compressibility, the application of an (isotropic) hydrostatic pressure leads to an area shrinkage at the expense of the volumetric bilayer thickness, in analogy to the osmotic pressure experiment (see above). However, the osmotic pressure mainly involves the transverse area contraction of the bilayer (pure shear), whereas the hydrostatic pressure experiment depends on both the area reduction as well as the longitudinal bilayer extension (both compression and pure shear).

Using the order parameters, we can then establish the correspondence of hydrostatic pressure to osmotic pressure for systems where the number of waters per lipid is known. Accordingly, Fig. 7 *a* presents plots of the segmental C$-^2$H order parameters for the plateau acyl chain segments of the DMPC-d_{54} bilayer in the liquid-crystalline (L_α) state for the three different ways of applying external pressure. One should recall that a larger value of S_{CD} indicates a thicker bilayer with a corresponding area reduction, and vice versa (49). First, we can see that by the criteria of ^{2}H NMR spectroscopy the effects of the dehydration and osmotic pressure are equivalent. They both produce approximately the same bilayer changes over the entire pressure range ($\approx 1-200$ atm). Second, the influence of hydrostatic pressure is clearly different and significant bilayer deformation occurs only at high values ($\approx 100-1000$ atm). But most striking, Fig. 7 *b* shows that we are able to unify all the results in terms of our approach. Here, the order parameters for the plateau acyl chain segments S_{CD}^{plat} are used to scale the osmotic pressure to the hydrostatic pressure giving a universal curve. The results are ≈superimposable regardless of whether the bilayer structural changes are brought about by gravimetric dehydration, by applying osmotic pressure, or by increased hydrostatic pressure. Hence, a common set of elastic constants explains bilayer interactions and deformation (strain) induced by an external force (stress) in all three cases (29,33).

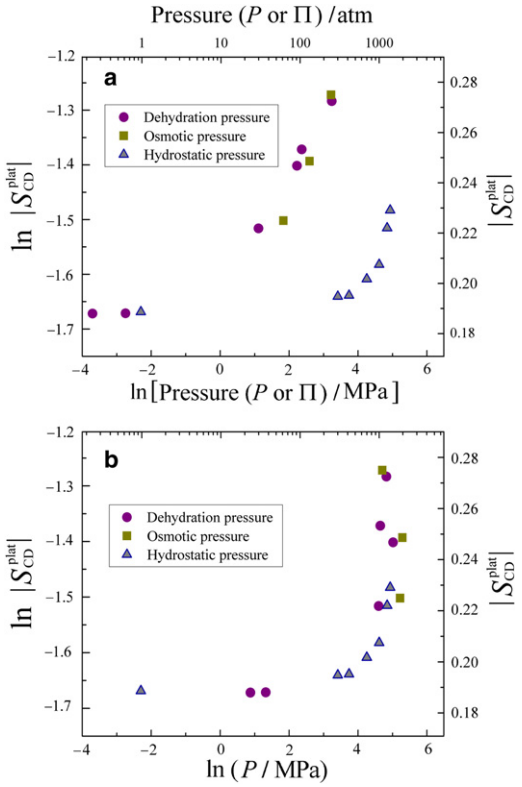

FIGURE 7 Comparison of structural changes due to applying external pressure in three different ways to DMPC-d_{54} membranes in the liquid-crystalline (L_α) state (see Fig. 1, *a*–*c*). (*a*) Order parameter $|S_{CD}^{plat}|$ for plateau acyl chain segments of DMPC-d_{54} at $T = 45°C$ plotted as a function of dehydration (gravimetric) pressure (●), osmotic pressure (■), and bulk hydrostatic pressure (▲). (*b*) The same data plotted as a function of hydrostatic pressure or equivalent osmotic pressure scaled by the order parameters (see Fig. 4). Note that solid-state ^{2}H NMR spectroscopy unifies the results for the various pressure-based measurements.

Bilayer deformation can influence membrane lipid-protein interactions

Last, we note that our results may have implications for the pressure sensitivity of membrane proteins. It is fascinating to recognize that the influences of osmotic pressure on lipid bilayer structure and dynamics are quite appreciable at values that clearly fall in the biological range. Significant influences of pressure have been attributed to direct effects of osmotic stress on membrane proteins, as in the case of mechanosensitive channels (68) and rhodopsin (13). However, the membrane lipid bilayer may also be sensitive to the osmotic pressure. The current ^{2}H NMR study supports the view that biomembranes are deformed by pressures $<100-200$ atm. Unanswered questions for future research include how the bilayer structural changes due to osmotic stress or hydrostatic pressure are related to membrane lysis by increasing area stretch; and whether feedback occurs between conformational changes of pressure-sensitive proteins and osmotically induced changes in bilayer structure via lipid-protein interactions.

SUPPORTING MATERIAL

Experimental methods, one figure, and one table are available at http://www.biophysj.org/biophysj/supplemental/S0006-3495(10)01379-2.

We thank V. A. Parsegian for discussions.

Financial support was provided by grants from the Indiana University-Purdue University Indianapolis Signature Center for Membrane Biosciences, the Arizona Biomedical Research Foundation, and the National Institutes of Health (grant Nos. EY012049 and EY018891).

REFERENCES

1. Tanford, C. 1980. The Hydrophobic Effect, 2nd Ed. John Wiley and Sons, New York.
2. White, S. H., and W. C. Wimley. 1999. Membrane protein folding and stability: physical principles. *Annu. Rev. Biophys. Biomol. Struct.* 28:319–365.
3. Dill, K. A., T. M. Truskett, …, B. Hribar-Lee. 2005. Modeling water, the hydrophobic effect, and ion solvation. *Annu. Rev. Biophys. Biomol. Struct.* 34:173–199.
4. Chandler, D. 2005. Interfaces and the driving force of hydrophobic assembly. *Nature.* 437:640–647.
5. Engelman, D. M. 2005. Membranes are more mosaic than fluid. *Nature.* 438:578–580.
6. Hessa, T., H. Kim, …, G. von Heijne. 2005. Recognition of transmembrane helices by the endoplasmic reticulum translocon. *Nature.* 433:377–381.
7. Bartels, D., and R. Sunkar. 2005. Drought and salt tolerance in plants. *Crit. Rev. Plant Sci.* 24:23–58.
8. Clegg, J. S. 2001. Cryptobiosis—a peculiar state of biological organization. *Comp. Biochem. Physiol. B.* 128:613–624.
9. Fu, D., A. Libson, …, R. M. Stroud. 2000. Structure of a glycerol-conducting channel and the basis for its selectivity. *Science.* 290:481–486.
10. Sukharev, S., M. Betanzos, …, H. R. Guy. 2001. The gating mechanism of the large mechanosensitive channel MscL. *Nature.* 409:720–724.
11. Kung, C. 2005. A possible unifying principle for mechanosensation. *Nature.* 436:647–654.
12. Mitchell, D. C., and B. J. Litman. 1999. Effect of protein hydration on receptor conformation: decreased levels of bound water promote metarhodopsin II formation. *Biochemistry.* 38:7617–7623.
13. Mitchell, D. C., and B. J. Litman. 2000. Effect of ethanol and osmotic stress on receptor conformation. Reduced water activity amplifies the effect of ethanol on metarhodopsin II formation. *J. Biol. Chem.* 275: 5355–5360.
14. Brown, M. F. 1982. Theory of spin-lattice relaxation in lipid bilayers and biological membranes. ^{2}H and ^{14}N quadrupolar relaxation. *J. Chem. Phys.* 77:1576–1599.
15. Lindahl, E., and O. Edholm. 2000. Mesoscopic undulations and thickness fluctuations in lipid bilayers from molecular dynamics simulations. *Biophys. J.* 79:426–433.
16. Brown, M. F. 1994. Modulation of rhodopsin function by properties of the membrane bilayer. *Chem. Phys. Lipids.* 73:159–180.
17. Perozo, E., and D. C. Rees. 2003. Structure and mechanism in prokaryotic mechanosensitive channels. *Curr. Opin. Struct. Biol.* 13:432–442.
18. Botelho, A. V., T. Huber, …, M. F. Brown. 2006. Curvature and hydrophobic forces drive oligomerization and modulate activity of rhodopsin in membranes. *Biophys. J.* 91:4464–4477.
19. Soubias, O., W. E. Teague, Jr., …, K. Gawrisch. 2010. Contribution of membrane elastic energy to rhodopsin function. *Biophys. J.* 99: 817–824.
20. Luzzati, V. 1968. X-ray diffraction studies of lipid-water systems. *In* Biological Membranes. D. Chapman, editor. Academic Press, New York. 71–123.

21. Mallikarjunaiah, K. J., A. Leftin, …, M. F. Brown. 2010. Osmotic membrane deformation revealed by solid-state ^{2}H NMR and small-angle x-ray scattering. *Biophys. J.* 98:282a.
22. Koenig, B. W., H. H. Strey, and K. Gawrisch. 1997. Membrane lateral compressibility determined by NMR and x-ray diffraction: effect of acyl chain polyunsaturation. *Biophys. J.* 73:1954–1966.
23. Skanes, I. D., J. Stewart, …, M. R. Morrow. 2006. Effect of chain unsaturation on bilayer response to pressure. *Phys. Rev. E.* 74: 051913-1–051913-8.
24. Eisenblätter, J., and R. Winter. 2006. Pressure effects on the structure and phase behavior of DMPC-gramicidin lipid bilayers: a synchrotron SAXS and ^{2}H-NMR spectroscopy study. *Biophys. J.* 90:956–966.
25. Singh, H., J. Emberley, and M. R. Morrow. 2008. Pressure induces interdigitation differently in DPPC and DPPG. *Eur. Biophys. J.* 37: 783–792.
26. Israelachvili, J., and H. Wennerström. 1996. Role of hydration and water structure in biological and colloidal interactions. *Nature.* 379: 219–225.
27. McIntosh, T. J., S. Advani, …, S. A. Simon. 1995. Experimental tests for protrusion and undulation pressures in phospholipid bilayers. *Biochemistry.* 34:8520–8532.
28. McIntosh, T. J., and S. A. Simon. 1986. Hydration force and bilayer deformation: a reevaluation. *Biochemistry.* 25:4058–4066.
29. Parsegian, V. A., N. Fuller, and R. P. Rand. 1979. Measured work of deformation and repulsion of lecithin bilayers. *Proc. Natl. Acad. Sci. USA.* 76:2750–2754.
30. Rand, R. P., and V. A. Parsegian. 1989. Hydration forces between phospholipid bilayers. *Biochim. Biophys. Acta.* 988:351–376.
31. McIntosh, T. J., A. D. Magid, and S. A. Simon. 1987. Steric repulsion between phosphatidylcholine bilayers. *Biochemistry.* 26:7325–7332.
32. Lis, L. J., M. McAlister, …, V. A. Parsegian. 1982. Interactions between neutral phospholipid bilayer membranes. *Biophys. J.* 37: 657–665.
33. McIntosh, T. J., and S. A. Simon. 1986. Area per molecule and distribution of water in fully hydrated dilauroylphosphatidylethanolamine bilayers. *Biochemistry.* 25:4948–4952.
34. Kenworthy, A. K., S. A. Simon, and T. J. McIntosh. 1995. Structure and phase behavior of lipid suspensions containing phospholipids with covalently attached poly(ethylene glycol). *Biophys. J.* 68:1903–1920.
35. Nagle, J. F., and S. Tristram-Nagle. 2000. Structure of lipid bilayers. *Biochim. Biophys. Acta.* 1469:159–195.
36. Petrache, H. I., and M. F. Brown. 2007. X-ray scattering and solid state deuterium nuclear magnetic resonance probes of structural fluctuations in lipid membranes. *In* Methods in Molecular Biology. A. M. Dopico, editor. Humana, Totowa, NJ. 341–353.
37. Simon, S. A., S. Advani, and T. J. McIntosh. 1995. Temperature dependence of the repulsive pressure between phosphatidylcholine bilayers. *Biophys. J.* 69:1473–1483.
38. Petrache, H. I., N. Gouliaev, …, J. F. Nagle. 1998. Interbilayer interactions from high-resolution x-ray scattering. *Phys. Rev. E.* 57:7014–7024.
39. McIntosh, T. J., and S. A. Simon. 1994. Hydration and steric pressures between phospholipid bilayers. *Annu. Rev. Biophys. Biomol. Struct.* 23:27–51.
40. Nagle, J. F., R. T. Zhang, …, R. M. Suter. 1996. X-ray structure determination of fully hydrated L_α phase dipalmitoylphosphatidylcholine bilayers. *Biophys. J.* 70:1419–1431.
41. Ly, H. V., and M. L. Longo. 2004. The influence of short-chain alcohols on interfacial tension, mechanical properties, area/molecule, and permeability of fluid lipid bilayers. *Biophys. J.* 87:1013–1033.
42. Brown, M. F. 1996. Membrane structure and dynamics studied with NMR spectroscopy. *In* Biological Membranes. A Molecular Perspective from Computation and Experiment. K. Merz, Jr. and B. Roux, editors. Birkhäuser, Basel, Switzerland. 175–252.
43. Petrache, H. I., A. Salmon, and M. F. Brown. 2001. Structural properties of docosahexaenoyl phospholipid bilayers investigated by solid-state ^{2}H NMR spectroscopy. *J. Am. Chem. Soc.* 123:12611–12622.
44. Brown, M. F., R. L. Thurmond, …, K. Beyer. 2001. Composite membrane deformation on the mesoscopic length scale. *Phys. Rev. E.* 64:010901-1–010901-4.
45. Pastor, R. W., R. M. Venable, and S. E. Feller. 2002. Lipid bilayers, NMR relaxation, and computer simulations. *Acc. Chem. Res.* 35: 438–446.
46. Leftin, A., and M. F. Brown. 2010. An NMR database for simulations of membrane dynamics. *Biochim. Biophys. Acta.* In press.
47. Brown, A., I. Skanes, and M. R. Morrow. 2004. Pressure-induced ordering in mixed-lipid bilayers. *Phys. Rev. E.* 69:011913-1–011913-9.
48. McCabe, M. A., and S. R. Wassall. 1997. Rapid deconvolution of NMR powder spectra by weighted fast Fourier transformation. *Solid State Nucl. Magn. Reson.* 10:53–61.
49. Petrache, H. I., S. W. Dodd, and M. F. Brown. 2000. Area per lipid and acyl length distributions in fluid phosphatidylcholines determined by ^{2}H NMR spectroscopy. *Biophys. J.* 79:3172–3192.
50. Petrache Laboratory. http://www.iupui.edu/~lab59/lab59_v2/osmotic/archiveddata.html.
51. Martinez, G. V., E. M. Dykstra, …, M. F. Brown. 2002. NMR elastometry of fluid membranes in the mesoscopic regime. *Phys. Rev. E.* 66:050902-1–050902-4.
52. Martinez, G. V., E. M. Dykstra, …, M. F. Brown. 2004. Lanosterol and cholesterol-induced variations in bilayer elasticity probed by ^{2}H NMR relaxation. *Langmuir.* 20:1043–1046.
53. Janiak, M. J., D. M. Small, and G. G. Shipley. 1979. Temperature and compositional dependence of the structure of hydrated dimyristoyl lecithin. *J. Biol. Chem.* 254:6068–6078.
54. Barry, J. A., T. P. Trouard, …, M. F. Brown. 1991. Low-temperature ^{2}H NMR spectroscopy of phospholipid bilayers containing docosahexaenoyl (22:6ω3) chains. *Biochemistry.* 30:8386–8394.
55. Wymann, M. P., and R. Schneiter. 2008. Lipid signaling in disease. *Nat. Rev. Mol. Cell Biol.* 9:162–176.
56. Wiener, M. C., and S. H. White. 1992. Structure of a fluid dioleoylphosphatidylcholine bilayer determined by joint refinement of x-ray and neutron diffraction data. III. Complete structure. *Biophys. J.* 61: 434–447.
57. Hristova, K., and S. H. White. 1998. Determination of the hydrocarbon core structure of fluid dioleoylphosphocholine (DOPC) bilayers by x-ray diffraction using specific bromination of the double-bonds: effect of hydration. *Biophys. J.* 74:2419–2433.
58. Nagle, J. F., and S. Tristram-Nagle. 2000. Lipid bilayer structure. *Curr. Opin. Struct. Biol.* 10:474–480.
59. Rajamoorthi, K., H. I. Petrache, …, M. F. Brown. 2005. Packing and viscoelasticity of polyunsaturated ω-3 and ω-6 lipid bilayers as seen by ^{2}H NMR and x-ray diffraction. *J. Am. Chem. Soc.* 127:1576–1588.
60. Ulmius, J., H. Wennerström, …, G. Arvidson. 1977. Deuteron NMR studies of phase equilibria in a lecithin-water system. *Biochemistry.* 16:5742–5745.
61. Kar, L., E. Ney-Igner, and J. H. Freed. 1985. Electron spin resonance and electron-spin-echo study of oriented multilayers of L_α-dipalmitoylphosphatidylcholine water systems. *Biophys. J.* 48:569–595.
62. Rand, R. P. 1981. Interacting phospholipid bilayers: measured forces and induced structural changes. *Annu. Rev. Biophys. Bioeng.* 10: 277–314.
63. Cohen, J. A., R. Podgornik, …, V. A. Parsegian. 2009. A phenomenological one-parameter equation of state for osmotic pressures of PEG and other neutral flexible polymers in good solvents. *J. Phys. Chem. B.* 113:3709–3714.
64. Otten, D., M. F. Brown, and K. Beyer. 2000. Softening of membrane bilayers by detergents elucidated by deuterium NMR spectroscopy. *J. Phys. Chem. B.* 104:12119–12129.

65. Wiedmann, T. S., R. D. Pates, …, M. F. Brown. 1988. Lipid-protein interactions mediate the photochemical function of rhodopsin. *Biochemistry.* 27:6469–6474.

66. Chang, G., R. H. Spencer, …, D. C. Rees. 1998. Structure of the MscL homolog from *Mycobacterium tuberculosis*: a gated mechanosensitive ion channel. *Science.* 282:2220–2226.

67. Abdine, A., M. A. Verhoeven, …, D. E. Warschawski. 2010. Structural study of the membrane protein MscL using cell-free expression and solid-state NMR. *J. Magn. Reson.* 204:155–159.

68. Perozo, E., A. Kloda, …, B. Martinac. 2002. Physical principles underlying the transduction of bilayer deformation forces during mechanosensitive channel gating. *Nat. Struct. Biol.* 9:696–703.

69. Powl, A. M., J. M. East, and A. G. Lee. 2008. Importance of direct interactions with lipids for the function of the mechanosensitive channel MscL. *Biochemistry.* 47:12175–12184.

70. Kodama, M., M. Abe, …, H. Takahashi. 2004. Estimation of interlamellar water molecules in sphingomyelin bilayer systems studied by DSC and x-ray diffraction. *Thermochim. Acta.* 416:105–111.

71. Pfeiffer, H., G. Klose, and K. Heremans. 2010. Thermodynamic and structural behavior of equimolar POPC/C_nE_4 ($n = 8$, 12, 16) mixtures by sorption gravimetry, ^{2}H NMR spectroscopy and x-ray diffraction. *Chem. Phys. Lipids.* 163:318–328.

72. Xu, W., and F. Pincet. 2010. Quantification of phase transitions of lipid mixtures from bilayer to non-bilayer structures: model, experimental validation and implication on membrane fusion. *Chem. Phys. Lipids.* 163:280–285.

73. Parsegian, V. A., R. P. Rand, …, D. C. Rau. 1986. Osmotic stress for the direct measurement of intermolecular forces. *Methods Enzymol.* 127:400–416.

74. Petrache, H. I., S. Tristram-Nagle, and J. F. Nagle. 1998. Fluid phase structure of EPC and DMPC bilayers. *Chem. Phys. Lipids.* 95:83–94.

75. Tristram-Nagle, S., H. I. Petrache, and J. F. Nagle. 1998. Structure and interactions of fully hydrated dioleoylphosphatidylcholine bilayers. *Biophys. J.* 75:917–925.

76. Finer, E. G., and A. Darke. 1974. Phospholipid hydration studied by deuteron magnetic resonance spectroscopy. *Chem. Phys. Lipids.* 12:1–16.

77. Bechinger, B., and J. Seelig. 1991. Conformational changes of the phosphatidylcholine headgroup due to membrane dehydration. A ^{2}H-NMR study. *Chem. Phys. Lipids.* 58:1–5.

78. Petrache, H. I., S. Tristram-Nagle, …, J. F. Nagle. 2004. Structure and fluctuations of charged phosphatidylserine bilayers in the absence of salt. *Biophys. J.* 86:1574–1586.

79. Högberg, C. J., and A. P. Lyubartsev. 2006. A molecular dynamics investigation of the influence of hydration and temperature on structural and dynamical properties of a dimyristoylphosphatidylcholine bilayer. *J. Phys. Chem. B.* 110:14326–14336.

80. Finer, E. G. 1973. Interpretation of deuteron magnetic resonance spectroscopic studies of hydration of macromolecules. *J. Chem. Soc., Faraday Trans. II.* 69:1590–1600.

81. Mills, I., T. Cvitaš, …, N. Kallay. 1993. IUPAC Quantities, Units and Symbols in Physical Chemistry. Blackwell Science, Oxford, UK.

82. Bonev, B. B., and M. R. Morrow. 1995. Hydrostatic pressure-induced conformational changes in phosphatidylcholine headgroups: a ^{2}H NMR study. *Biophys. J.* 69:518–523.